Inorg. Chem. **2005**, *44*, 7511–7522

NMR Investigation of the Interaction of Vanadate with Carbasilatranes in Aqueous Solutions

Evgenios M. Evgeniou,[†] Spyros A. Pergantis,[‡] Epameinondas Leontidis,[†] and Anastasios D. Keramidas*,[†]

Departments of Chemistry, University of Cyprus, 1678 Nicosia, Cyprus, and University of Crete, 71409 Heraklion, Greece

Received June 9, 2005

Reaction of vanadate with carbasilatranes [methoxy{*N*,*N*′,*N*″-2,2′,3-[bis(1-methylethanolato)(propyl)]amino}silane (**1**), methoxy{*N*,*N*′,*N*″-2,2′,3-[bis(1-ethanolethanolato)(propyl)]amino}silane (**2**), and {*N*,*N*′,*N*″-2,2′,2-[bis(ethanolato)-(glycolpropyl ether)]amino}silane (**3**)] in aqueous solution results in the formation of vanadosilicates and five-coordinated chelate vanadium(V) complexes as evidenced by ^{51}V, ^{1}H, and ^{13}C NMR spectroscopy. Chiral carbasilatrane *S*,*S*-**1** was characterized in the solid state by X-ray diffraction, revealing a trigonal bipyramidal geometry around the metal ion, with one unidentate methoxy group and one atrane nitrogen atom at the axial positions and one carbon and two atrane oxygen atoms at the equatorial plane of the bipyramid. Crystal data (Mo Kα; 100(2) K) are as follows: orthorhombic space group $P2_12_12_1$; $a = 8.8751(6)$, $b = 9.7031(7)$, $c = 14.2263(12)$ Å; $Z = 4$. The complexation of vanadium either with **1** or **2** is stereoselective yielding ~94% of the complex containing ligand in the *S*,*R*-configuration. The lower ability of the *S*,*S*- and *R*,*R*-diastereoisomers of **1** and **2** to ligate vanadate was attributed to stereochemical factors, dictating a square pyramidal geometry for the chelated complexes. A dynamic process between the vanadium chelate complexes and the respective carbasilatranes was evaluated by 2D {^{1}H} EXSY NMR spectroscopy. These spectra show that the vanadate complexes with the open carbasilatranes exchange more slowly with the free ligand compared to the respective alcohol aminate complexes.

Introduction

The development of environmentally friendly technologies has prompted much research in heterogeneous catalysis and in the heterogenization of known active homogeneous catalysts for oxidation.[1,2] The heterogenization approach constitutes a convenient marriage of the engineering advantages of heterogeneous catalysts, such as ease of recovery, with advantageous features of homogeneous catalysts, such as better selectivity and higher tunability.[3,4] Inorganic materials such as silica are particularly suitable as heterogeneous catalyst supports because of their high mechanical strength and chemical inertness. In addition, the production of silicon-based inorganic oxides through solution chemical techniques, such as the sol−gel process, is an ideal method for catalyst immobilization because of its diversity and mildness.[5] Transition metal ions can be introduced into oxide gels produced by the sol−gel method, either at the sol stage or after the gel is formed by posttreatment and surface derivatization. The former method is particularly attractive due to the generation of several catalytic metal centers uniformly distributed into the bulk of the silica matrix. Hydrolysis and condensation reactions produce an inorganic or a hybrid organic−inorganic xerogel incorporating a metal complex. The metal ions dissolved in the sol rearrange the local structure of the gel to suit their bonding requirements, thus forming complexes of various coordination numbers. Several key properties of the final material arise from the nature of the metal ion sites distributed within the silica matrix. Consequently, the detailed study of the chemistry occurring in the sol solutions is essential because it will provide

* To whom correspondence should be addressed. E-mail: akeramid@ucy.ac.cy. Fax: (357)22892801.
[†] University of Cyprus.
[‡] University of Crete.

(1) Price, P. M.; Clark, J. H.; Macquarrie, D. J. *J. Chem. Soc., Dalton Trans.* **2000**, 101.
(2) Xia, Q.-H.; Ge, H.-Q.; C.-P.; Y.; Liu, Z.-M.; Su, K.-X. *Chem. Rev.* **2005**, *105*, 1603.
(3) Corma, A.; Garcia, H. *Chem. Rev.* **2002**, *102*, 3837.
(4) Wight, A. P.; Davis, M. E. *Chem. Rev.* **2002**, *102*, 3589.
(5) Lindner, E.; Schneller, T.; Auer, F.; Mayer, H. A. *Angew. Chem., Int. Ed.* **1999**, *116*, 348.

10.1021/ic050929q CCC: $30.25
Published on Web 09/20/2005

information, at the molecular level, for the chemical processes which give rise to the gel properties.

In this work we develop silicate-based vanadium complexes with the view to produce heterogeneous catalysts for stereoselective and enantioselective oxidations of organic substrates. Inspired by the studies of the structure and function of vanadium(V) haloperoxidases, several research groups have applied vanadium(V) complexes to the homogeneous peroxidative oxidation of alkenes, aromatic hydrocarbons, and alkanes and to sulfoxidation.[6−21] Ligation of vanadate with organic ligands was shown to increase stereoselectivity in oxidation reactions. For example vanadate complexes with alcohol−aminate ligands (e.g. {VO[N(CH_2-$CH_2O)_3$]}) oxidized benzene and cyclohexane with significant stereoselectivity.[9] Introduction of chiral centers into the alcohol−aminate ligands (R′N($CH_2CHROH)_2$, R = −Me or −Ph) was found to yield enantioselective catalysts for sulfoxidation reactions.[18]

Molecules containing amino−alcoholic groups covalently attached to alkoxy silanes might be very useful for the synthesis of immobilized stereoselective and enantioselective oxygen transfer catalysts based on vanadium(V). Carbasilatranes,[22] which satisfy the above structural criteria, have lower hydrolytic rates than alkoxy silanes giving a better control of the sol−gel polymerization process.[23] A disadvantage of these compounds might be the high affinity of amino−alcohols to ligate silicon(IV), which thus competes with vanadate for the ligation of the chelate moiety. Further complications might arise in the sol−gel solutions from the strong interactions between vanadate and silicates, which lead to the formation of V−O−Si bonds. Although vanadium(V) is well-known to combine with silicates,[24] in particular in mesoporous silicas,[25] there is only one report on simple aqueous vanadosilicates,[26] whereas no reports have been published to date related to the interaction of carbasilatranes with vanadate or its oligomers.

In this study, we characterized the species generated from the reaction of vanadate with carbasilatranes [(methoxy-{*N*,*N*′,*N*″-2,2′,3-[bis(1-methylethanolato)(propyl)]amino}-silane (**1**), methoxy{*N*,*N*′,*N*″-2,2′,3-[bis(1-ethanolethanolato)-(propyl)]amino}silane (**2**), and methoxy{*N*,*N*′,*N*″-2,2′,2-[bis(ethanolato)(glycolpropyl ether)]amino}silane) (**3**)] in aqueous solution using multinuclear NMR spectroscopy. The stability and the stereochemistry of the chelate complexes in solution are controlled by steric interactions between the substituents on the chelate rings of amino−alcohols. We anticipate that this study will facilitate the development of useful stereoselective immobilized oxidation catalysts in situations where both the catalytic properties of transition metal ions and the presence of a silica matrix are required.

Experimental Section

Materials and Methods. The reactions for the synthesis of silatranes were performed under high-purity argon using standard Schlenk techniques. All solvents used in this study except methanol were dried over CaH_2 and distilled before use. Methanol was dried with CH_3ONa. $NaVO_3$, (3-aminopropyl)trimethoxysilane, (3-glycidoxypropyl)trimethoxysilane, *R*- and *S*-optical isomers of propylene oxide, glycidol, *N*-[3-trimethoxysilyl)propyl]ethylenediamine, and propylamine were purchased from Aldrich and used without further purification. Propylene oxide and diethanolamine were purchased from Aldrich and were dried over CaH_2. Elemental analyses were performed on a EuroVector 3000 CHN analyzer.

Synthesis of Methoxy{*N*,*N*′,*N*″-2,2′,3-[bis(1-methylethanolato)-(propyl)]amino}silane (1). This compound was prepared by a modified literature procedure.[22] Propylene oxide (32.0 mL, 460 mmol) was added to a stirred solution of (3-aminopropyl)-trimethoxysilane (40.0 mL, 230 mmol) in MeOH (100 mL). The mixture was refluxed for 2 days. The solvent was removed under reduced pressure, and the colorless oily residue was redissolved in hot dry hexane. The solution was refrigerated overnight, and the resulting white crystalline precipitate was filtered out. The solid was collected and recrystallized with hot hexane (25 mL) affording 41.0 g (77%) of white crystals of **1**. ^{1}H NMR [δ ($CDCl_3$) (ppm)]: *S*,*S*-**1** and *R*,*R*-**1**, 2.32 (m, H_{1a}, J_{1a-1b} = 12.2 Hz, J_{1a-2a} = 4.90 Hz, J_{1a-2b} = 13.5 Hz), 2.79 (m, H_{1b}, J_{1b-2a} = 1.60 Hz, J_{1b-2b} = 4.98 Hz), 1.68 (m, H_{2a}, J_{2a-2b} = 14.4 Hz, J_{2a-3b} = 1.60 Hz), 1.55 (m, H_{2b}, J_{2b-3b} = 5.80 Hz), 0.49 (m H_{3a}, J_{3a-3b} = 15.6 Hz, J_{3a-2a} = 7.94 Hz, J_{3a-2b} = 12.9 Hz), 0.80 (m, H_{3b}, J_{3b-1b} = 1.30 Hz), 2.21 (t, H_{4a}, J_{4a-4b} = 12.3 Hz), 2.75 (m, H_{4b}), 2.20 (t, H_{5a}, J_{5a-5b} = 12.3 Hz), 2.68 (d, H_{5b}), 3.86 (m, H_6, J_{6-4a} = 11.1 Hz, J_{6-4b} = 3.72 Hz, J_{6-8} = 6.08 Hz), 3.96 (m, H_7, J_{7-5a} = 11.1 Hz, J_{7-5b} = 3.72 Hz, J_{7-9} = 6.08 Hz), 1.18 (d, $3H_8$), 1.17 (d, $3H_9$), 3.41 (s, $3H_{10}$); *S*,*R*-**1**, 2.66 (d, 2H, H_1, J_{1-2} = 12.4 Hz), 1.67 (m, 2H, H_2, J_{2-3} = 7.02 Hz), 0.71 (t, 2H, H_3), 2.43 (q, H_{4a}, H_{5a}, J_{4a-4b} = 12.6 Hz, J_{5a-5b} = 12.6 Hz), 2.95 (q, H_{4b}, H_{5b}), 4.03 (m, 2H,H_6,H_7, J_{6-4a} = 8.68 Hz, J_{6-4b} = 5.0 Hz, J_{6-8} = 6.2 Hz,, J_{7-5a} = 8.68 Hz, J_{7-5b} = 5.0 Hz, J_{7-9} = 6.2 Hz), 1.21 (d, 6H,$3H_8$, $3H_9$), 3.44 (s, $3H_{10}$). *R*,*S*-**1**: 2.72 (d, 2H, H_1, J_{1-2} = 12.4 Hz), 1.70 (m, 2H, H_2, J_{2-3} = 7.06 Hz), 0.72 (t, 2H, H_3), 2.46 (q, H_{4a}, H_{5a}, J_{4a-4b} = 12.6 Hz, J_{5a-5b} = 12.6 Hz), 2.85 (q, H_{4b}, H_{5b}), 4.16 (m, 2H,H_6,H_7, J_{6-4a} = 8.68 Hz, J_{6-4b} = 5.0 Hz, J_{6-8} = 6.2 Hz, J_{7-5a} = 8.68 Hz, J_{7-5b} = 5.0 Hz, J_{7-9} = 6.2 Hz), 1.22 (d, 6H,$3H_8$, $3H_9$), 3.43 (s, $3H_{10}$). ^{13}C NMR [δ ($CDCl_3$) (ppm)]: *S*,*S*-**1** and *R*,*R*-**1**, 53.27 (C_1), 21.0 (C_2), 8.24 (C_3), 60.18 (C_4), 60.18 (C_5), 64.59 (C_6), 64.96 (C_7), 20.69 (C_8), 20.69 (C_9),

(6) Bonchio, M.; Conte, V.; Di Furia, F.; Modena, G. *J. Org. Chem.* **1989**, *54*, 4368.
(7) Sharpless, K. B.; Michaelson, R. C. *J. Am. Chem. Soc.* **1973**, *95*, 6136.
(8) Murase, N.; Hoshino, Y.; Oishi, M.; Yamamoto, H. *J. Org. Chem.* **1999**, *64*, 338.
(9) Reis, P. M.; Silva, J. A. L.; Silva, J. J. R. F.; Pombeiro, A. J. L. *Chem. Commun.* **2000**, 1845.
(10) Colpas, G. J.; Hamstra, B. J.; Kampf, J. W.; Pecoraro, V. L. *J. Am. Chem. Soc.* **1996**, *118*, 3469.
(11) Butler, A.; Clague, M. J.; Meister, G. E. *Chem. Rev.* **1994**, *94*, 625.
(12) Rehder, D. *Coord. Chem. Rev.* **1999**, *182*, 297.
(13) Mimoum, H.; Saussine, L.; Daire, E.; Postel, M.; Fischer, J.; Weiss, R. *J. Am. Chem. Soc.* **1983**, *105*, 3101.
(14) Hamstra, B. J.; Colpas, G. J.; Pecoraro, V. L. *Inorg. Chem.* **1998**, *37*, 949.
(15) Suss-Fink, G.; Stanislas, S.; Shul'pin, G. B.; Nizova, G. V.; Stoelki-Evans, H.; Neels, A.; Bobillier, C.; Claude, S. *J. Chem. Soc., Dalton Trans.* **1999**, 3169.
(16) Shilov, A. E.; Shul'pin, G. B. *Chem. Rev.* **1997**, *97*, 2879.
(17) Hirao, T. *Chem. Rev.* **1997**, *97*, 2707.
(18) Santoni, G.; Licini, G.; Rehder, D. *Chem.−Eur. J.* **2003**, *9*, 4700.
(19) Blaser, H. U. *Chem. Rev.* **1992**, *92*, 935.
(20) Kagan, H. B.; Riant, O. *Chem. Rev.* **1992**, *92*, 1007.
(21) Maurya, M. R.; Agrwal, S.; Bader, C.; Rehder, D. *Eur. J. Inorg. Chem.* **2005**, 147.
(22) Morehouse, E. L. U.S. Patent 3,032,576, 1962.
(23) Phiriyawirut, P.; Jamieson, A. M.; Woughasemsit, S. *Microporous Mesoporous Mater.* **2005**, *77*, 203.
(24) Wang, X.; Liu, L.; Zhang, G.; Jacobson, A. J. *Chem. Commun.* **2001**, 2472.
(25) Gontier, S.; Tuel, A. *Microporous Mater.* **1995**, *5*, 161.
(26) Howarth, O. W.; Hastings, J. J. *J. Chem. Soc., Dalton Trans.* **1996**, 4189.

Chart 1. Numbering and Configurations of Diastereoisomers **1**−**4**

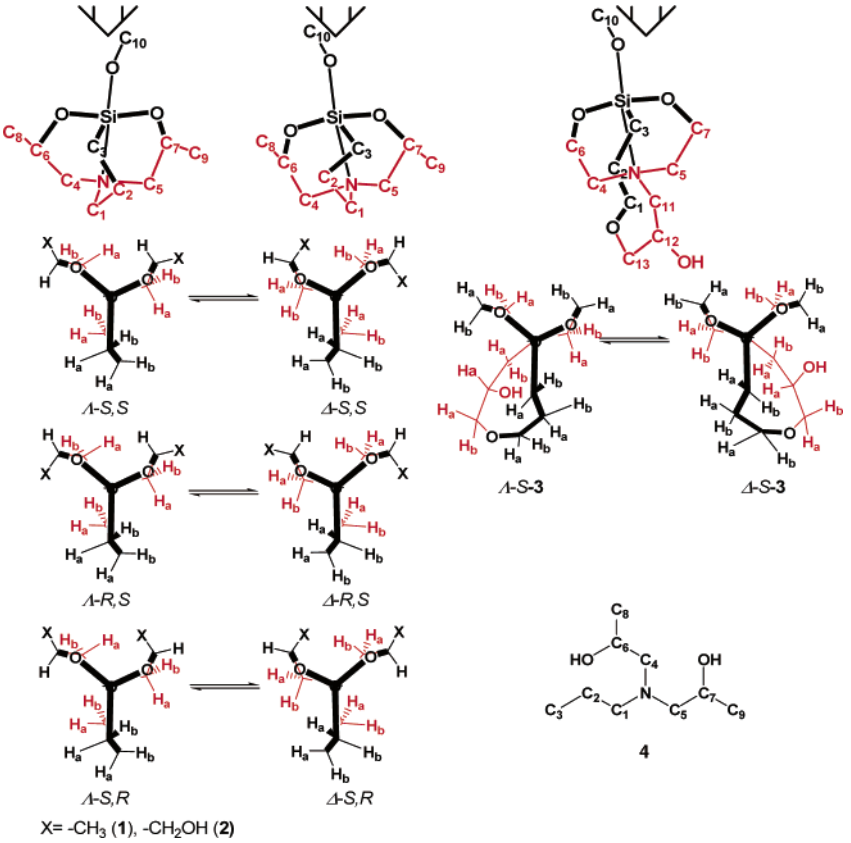

50.28 (C_{10}). *S,R*-**1**: 56.21 (C_1), 22.69 (C_2), 7.84 (C_3), 65.06 (C_4, C_5), 67.13 (C_6, C_7), 22.78 (C_8, C_9), 50.45 (C_{10}); *R,S*-**1**, 59.41 (C_1), 22.1 (C_2), 9.82 (C_3), 63.19 (C_4, C_5), 67.71 (C_6, C_7), 22.39 (C_8, C_9), 50.11 (C_{10}). ^{29}Si NMR [δ ($CDCl_3$) (ppm)]: *S,S*-**1** and *R,R*-**1**, −63.8; *S,R*-**1**, −62.4; *R,S*-**1**, −61.4. The numbering is according to Chart 1. Anal. Calcd for $C_{10}H_{21}NO_3Si$: C, 51.91; H, 9.15; N, 6.05; Found: C, 51.90; H, 9.12; N, 6.11.

Synthesis of *S,S*-1. The reaction of (3-aminopropyl)trimethoxysilane (2.00 mL, 11.5 mmol) with (*S*)-(−)-propylene oxide (1.6 mL, 23 mmol) was carried out in a manner similar to that described for **1**. The mixture was refluxed for 2 days. The yield was 2.09 g (79%). ^{1}H, ^{13}C, and ^{29}Si NMR spectra of *S,S*-**1** in $CDCl_3$ gave exactly the same peaks as those of the *S,S*-**1** and *R,R*-**1** isomers of the racemic **1** described above.

Synthesis of *R,R*-1. This complex was prepared by a procedure analogous to that described for *S,S*-**1**, using (3-aminopropyl)-trimethoxysilane (2.00 mL, 11.5 mmol) and (*R*)-(+)-propylene oxide (1.6 mL, 23 mmol) as reactants. The yield was 2.05 g (77%). The compound gave NMR spectra identical with that of *S,S*-**1**.

Synthesis of Methoxy{*N,N′,N″*-2,2′,3-[bis(1-ethanolethanolato)-(propyl)]amino}silane (2). Glycidol (4.56 mL, 68.8 mmol) was added to a stirred solution of (3-aminopropyl)trimethoxysilane (6.00 mL, 34.4 mmol) in MeOH (15 mL) at room temperature. The mixture was refluxed for 2 days. The solvent was removed under reduced pressure, and the colorless residue was redissolved in hot CH_3CN. The solution was refrigerated overnight. The resulting white crystalline precipitate was filtered out, washed with hot hexane (10 mL), and dried under vacuum. The yield was 4.3 g (46%). ^{1}H NMR [δ ($CDCl_3$) (ppm)]: *S,S*-**2** and *R,R*-**2**, 2.36 (d, H_{1a}, J_{1a-1b} = 12.0 Hz, $J_{1a\ -2a}$ = 4.82 Hz, J_{1a-2b} = 13.3 Hz), 2.96 (t, H_{1b}, J_{1b-2a} = 1.1 Hz, J_{1b-2b} = 4.82 Hz), 1.92 (m, H_{2a}, J_{2a-2b} = 14.4 Hz, J_{2a-3a} = 7.8 Hz, J_{2a-3b} = 1.2 Hz), 1.68 (m, H_{2b}, J_{2b-3a} = 12.1 Hz, J_{2b-3b} = 6.02 Hz), 1.14 (m, H_{3a}, J_{3a-3b} = 15.7 Hz), 0.62 (m, H_{3b}), 2.72 (m,4H, $2H_4$, $2H_5$), 3.89 (m, H_6, J_{6-8a} = 3.61 Hz, J_{6-8b} = 2.41 Hz), 4.27 (m, H_7, J_{7-9a} = 3.61 Hz, J_{7-9b} = 2.41 Hz), 3.46 (d, $3H_{8a}$, J_{8a-8b} = 12.1 Hz), 3.41 (d, H_{8b}), 3.66 (q, H_{9a}, J_{9a-9b} = 12.1 Hz), 3.77 (q, H_{9b}), 3.38 (d, $3H_{10}$). *S,R*-**2**: 2.95 (m, 2H, H_1, J_{1-2} = 11.6 Hz), 1.77 (m, 2H, H_2, J_{2-3} = 7.15 Hz), 0.52 (d, 2H, H_3), 2.84 (d, 2H, H_4), 2.85 (d, 2H, H_5), 4.28 (m, 2H,H_6,H_7, J_{6-4} = 8.43 Hz, J_{6-8a} = 4.82 Hz, J_{6-8b} = 3.61 Hz, J_{7-5} = 6.01 Hz, J_{7-9a} = 3.61 Hz, J_{7-9b} = 4.82 Hz), 3.47 (d, H_{8a}, J_{8a-8b} = 10.8 Hz), 3.42 (d, H_{8b}), 3.85 (d, H_{9a}, J_{9a-9b} = 10.8 Hz), 3.78 (d, H_{9b}), 3.39 (s, $3H_{10}$); *R,S*-**2**, 2.95 (m, 2H, H_1, J_{1-2} = 12.3 Hz), 1.83 (m, 2H, H_2, J_{2-3} = 7.11 Hz), 0.56 (d, 2H, H_3), 2.83 (d, 2H, H_4), 2.84 (d, 2H, H_5), 4.47 (m, 2H, H_6,H_7, J_{6-4} = 6.01 Hz, J_{6-8a} = 3.61 Hz, J_{6-8b} = 4.82 Hz, J_{7-5} = 8.43 Hz, J_{7-9a} = 4.82 Hz, J_{7-9b} = 3.61 Hz), 3.46 (d, H_{8a}, J_{8a-8b} = 10.8 Hz), 3.44 (d, H_{8b}), 3.78 (d, H_{9a}, J_{9a-9b} = 10.8 Hz), 3.73 (d, H_{9b}), 3.39 (s, $3H_{10}$). ^{13}C NMR [δ ($CDCl_3$) (ppm)]: *S,S*-**2** and *R,R*-**2**, 53.52 (C_1), 20.64 (C_2), 7.87 (C_3), 54.25 (C_4), 54.09 (C_5), 63.89 (C_6), 64.10 (C_7), 69.02 (C_8), 69.42 (C_9), 50.26 (C_{10}); *S,R*-**2**, 56.04 (C_1), 22.06 (C_2), 7.47 (C_3), 58.13 (C_4, C_5), 64.61 (C_6, C_7), 71.42 (C_8,C_9), 50.26 (C_{10}); *R,S*-2, 59.01 (C_1), 22.50 (C_2), 9.37 (C_3), 57.44 (C_4, C_5), 64.79 (C_6, C_7), 72.00 (C_8, C_9), 50.60 (C_{10}). ^{29}Si NMR [δ ($CDCl_3$) (ppm)]: *S,S*-**2** and *R,R*-**2**, −63.6; *S,R*-**2**, −62.6; *R,S*-**2**, −60.8. The numbering is according to Chart 1. Anal. Calcd for $C_{10}H_{21}NO_5Si$: C, 45.61; H, 8.04; N, 5.32. Found: C, 45.21; H, 8.11; N, 5.41.

Synthesis of Methoxy{*N,N′,N″*-2, 2′,2-[bis(ethanolato)(glycolpropyl ether)]amino}silane (3). (3-Glycidoxypropyl)trimethoxysilane (20.0 mL, 90.5 mmol) was added to a stirred solution of diethanolamine (9.80 g, 90.5 mmol) in MeOH (25 mL). The mixture was refluxed for 6 days. Dry MeOH (30 mL) was added resulting in a clear and colorless solution. After 1 day at 273 K a white solid was formed. The precipitate was filtered out, washed with

hexane, and dried under vacuum. The yield was 17.5 g (70%). ^{1}H NMR [δ ($CDCl_3$) (ppm)]: 3.37 (m, 2H, H_1, $J_{1-2} = 16.4$ Hz), 1.56 (m, 2H, H_2, $J_{2-3} = 16.4$ Hz), 0.26 (m, 2H, H_3), 3.71 (m, 4H, H_4, H_5), 2.79 (m, 4H, H_6, H_7), 3.46 (s, $3H_{10}$), 2.48 (m, H_{11a}, $J_{11a-11b} = 11.7$ Hz, $J_{11a-12} = 11.7$ Hz), 2.96 (m, H_{11b}, $J_{11b-12} = 4.14$ Hz), 3.92 (m, 1H, H_{12}), 3.61 (t, H_{13a}, $J_{13a-13b} = 11.7$ Hz, $J_{13a-12} = 8.19$ Hz), 3.31 (m, H_{13b}, $J_{13b-12} = 4.14$ Hz). ^{13}C NMR [δ ($CDCl_3$) (ppm)]: 75.67 (C_1), 25.64 (C_2), 12.64 (C_3), 58.03 (C_4, C_5), 52.33 (C_6), 51.82 (C_7), 51.06 (C_{10}), 54.79 (C_{11}), 66.84 (C_{12}), 73.49 (C_{13}). ^{29}Si NMR [δ ($CDCl_3$) (ppm)]: −68.0. The numbering is according to Chart 1. Anal. Calcd for $C_{11}H_{23}NO_5Si$: C, 47.63; H, 8.36; N, 5.05. Found: C, 47.44; H, 8.19; N, 5.14.

Synthesis of {[*N*,*N*-(Propyl)]amino}bis(propan-2-ol) (4). Propylene oxide (1.70 mL, 24.4 mmol) was added to a stirred solution of propylamine (1.00 mL, 12.2 mmol) in MeOH (15 mL). The mixture was refluxed for 7 days. The solvent was removed under reduced pressure, and the residue was redissolved in aqueous HCl (12 M, 10 mL). The solvent was evaporated until dry under reduced pressure, and the remaining brownish oil was redissolved in acetone (∼30 mL). *n*-Hexane (∼50 mL) was added into the solution until an oil was formed. The solvent was decanted, and the oil was washed with hot ethyl acetate providing a white solid. The solid was dried under vacuum. The yield was 1.10 g (43%). ^{1}H NMR [δ (D_2O)]: 3.23 (m, 6H, H_1, $H_{4,5}$), 1.75 (m, 2H, H_2), 0.97 (q, 3H, H_3), 4.22 (m, $H_{6,7}$), 1.24 (m, 3H, $H_{8,9}$). ^{13}C NMR [δ (D_2O) (ppm)]: 56.16 (C_1), 20.13 (C_2), 10.34 (C_3), 61.53 (C_4, C_5), 62.55 (C_6, $C_{7,}$), 20.59 (C_8, C_9). The numbering is according to Chart 1. Anal. Calcd for $C_9H_{21}NO_2$: C, 61.67; H, 12.08; N, 7.99. Found: C, 61.74; H, 12.19; N, 7.73.

Synthesis of *S*,*S*-{[*N*,*N*-(Propyl)]amino}bis(propan-2-ol) (*S*,*S*-4). This compound was prepared by a procedure analogous to that described for **4**, using propylamine (1.00 mL, 12.2 mmol) and (*S*)-(−)-propylene oxide (1.70 mL, 24.4 mmol). The yield was 1.7 g (66%). ^{1}H NMR [δ (D_2O)]: 3.23 (m, 6H, H_1, $H_{4,5}$), 1.76 (m, 2H, H_2), 0.97 (m, 3H, H_3), 4.18 (m, $H_{6,7}$), 1.25 (m, 3H, $H_{8,9}$). ^{13}C NMR [δ (D_2O) (ppm)]: 56.15 (C_1), 16.81 (C_2), 10.23 (C_3), 61.48 (C_4, C_5), 61.56 (C_6, C_7), 20.16 (C_8, C_9). The numbering is according to Chart 1.

Preparation of Vanadate−Carbasilatrane Aqueous Solutions. The vanadate−carbasilatrane solutions were prepared by mixing various amounts of standard solutions of $NaVO_3$ (1.500 M) and carbasilatranes (1.000 M) or the prehydrolyzed with acid carbasilatranes in deuterium oxide at pH ∼ 9. To reach equilibrium the solutions were kept at room temperature for 6 days and then the pH was corrected again. The composition of these solutions was checked by NMR spectroscopy.

The prehydrolyzed with acid standard solutions of silatranes (1.000 M) were prepared by adding trifluoroacetic acid (0.390 mL, 5.00 mmol) into an aqueous solution of silatrane (1.160 g, 5.000 mmol) in D_2O (5.000 mL). The clear solution was stirred for 3 h, and then the pH was adjusted to 7.0 by aqueous solutions of NaOD (0.01−0.50 M). All solutions for the NMR measurements were prepared in triplicates.

NMR Spectroscopy. NMR spectra were recorded on a Bruker Avance 300 spectrometer operating at 300, 75.5, 59.6, and 78.9 MHz for ^{1}H, ^{13}C, ^{29}Si, and ^{51}V nuclei, respectively. The ^{1}H, ^{13}C, ^{29}Si, and ^{51}V NMR spectra were recorded using a sweep width of 1000, 4500, 7000, and 30 000 Hz, respectively, and a 30° pulse. The exact chemical shifts, coupling constants, *J*, and integrals were calculated by simulation of the experimental spectra using the software gNMR.[27]

The 2D ^{1}H NMR COSY-45 (pulse sequence $90°-t_1-45°$) and 2D {^{13}C,^{1}H} HETCOR experiments were conducted using 256 increments (each consisting of 16 scans) covering the full spectrum (4.0 ppm in both dimensions and 4.0 ppm on F1 and 70 on F2 dimensions, respectively). The phase-sensitive HMQC sequence enriched with BIRD filter and GARP decoupling (90°) was applied at inverse H, C correlation for the 2D HMQC spectra. The standard NOESY pulse sequence ($90°-t_1-90°-t_m-90°$) was used in the 2D {^{1}H} EXSY−NOESY measurements, and these spectra were acquired using 512 increments (with 16 scan each) covering the full spectrum (4.0 ppm in both dimensions) and 0.20−0.35 s mixing time (t_m). The spectra were run with temperature control at 25, 50, 80, and 150 °C.

For the assignments of the different ^{29}Si NMR peaks we used the following terminology: each silicon atom is noted S_x^y with $0 < x + y < 3$, x and y being positive integers. S° refers to the monomers **1**−**3**, while x is the number of bridging oxygens and y the number of hydroxides on the silicon centers.

X-ray Structure Determination. Crystals suitable for X-ray diffraction study were obtained by recrystallization of *S*,*S*-**1** in *n*-hexane. The intensity data of *S*,*S*-**1** were collected on a XCalibur III, 4-cycle diffractometer ($\lambda = 0.7107$ Å). The structure was solved by direct methods using the program SHELX-86[28] and refined by full-matrix least-squares techniques.[29]

Mass Spectrometric Analysis. All electrospray mass spectrometric experiments were performed using an LCQ Advantage (ThermoElectron, San Jose, CA) mass spectrometer, equipped with a pneumatically assisted electrospray source and an ion trap mass analyzer with unit mass resolution and capable of conducting MS. In all experiments the ion source was operated in the positive ion mode. Instrument settings were optimized for maximum intensity of the expected molecular ions. Typical values for the electrospray ionization potential ranged from 4 to 5 kV, with transfer capillary temperatures ranging from 200 to 300 °C. Samples in solution were infused continuously into the electrospray source at a flow rate of 3 μL/min.

Results and Discussion

Synthesis. The silatranes **1**−**3** were synthesized in high yields (50−80%) by a modification of an older method.[22] The main difference in the new synthesis is the purification of the compounds **1**−**3** through recrystallization from *n*-hexane, CH_3CN, and CH_3OH, respectively, in contrast to the distillation process used previously. Reaction of (3-aminopropyl)trimethoxysilane with racemic epoxides gave all the possible combinations of isomers of **1** and **2** shown in Chart 1. Compound **3** was synthesized by the reaction of racemic (3-glycidoxypropyl)trimethoxysilane with diethanolamine. Chiral *S*,*S*-**1** (eq 1) and *R*,*R*-**1** were obtained from reaction of (3-aminopropyl)trimethoxy silane with *S*- and *R*-propylene oxide, respectively.

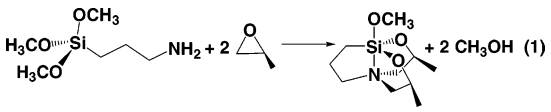

All compounds were very soluble in both water and organic solvents. The solids and the organic solutions of **1**

(27) Budzelaar, H. M. P. *gNMR version 4.1.0*; Cherwell Schientific Publishing: Oxford, U.K., 1999.

(28) Sheldrick, G. M. *SHELXS-86: Program for the Solution of Crystal Structure*; University of Gottingen: Gottingen, Germany, 1990.

(29) Sheldrick, G. M. *SHELXL-97: Program for the Refinement of Crystal Structure*; University of Gottingen: Gottingen, Germany, 1997.

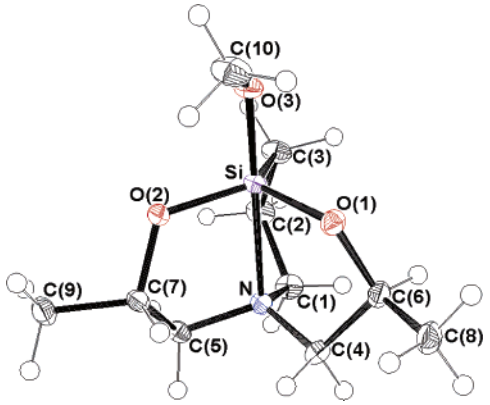

Figure 1. ORTEP drawing of Λ-*S*,*S*-**1** with 50% probability ellipsoids.

Table 1. Crystal and Structure Refinement Data for (*S*,*S*)-**1**

empirical formula	$C_{10}H_{21}NO_3Si$
cryst size (mm^3)	0.375 × 0.239 × 0.145
fw	231.37
temp (K)	100(2)
wavelength (Å)	0.710 73
cryst syst	orthorhombic
space group	$P2_12_12_1$
a (Å)	8.8751(6)
b (Å)	9.7031(7)
c (Å)	14.2263(12)
V ($Å^3$)	1225.11(16)
Z	4
ρ_{calcd} (Mg/m^3)	1.254
abs coeff (mm^{-1})	0.1814
θ range for data collcn (deg)	4.23−31.08
index ranges	$-12 \le h \le 12$, $-12 \le k \le 13$, $-20 \le l \le 19$
no. of obsd reflcns	8660
no. of indpdt reflcns	3586
data/params	16.3
max/min Δ*p* (e $Å^{-3}$)	0.348, −0.288
R, wR (obsd data)	0.0286, 0.0782
R, wR (all data)	0.0277, 0.0794

[a] Refinement method: full-matrix least squares on F^2.

and **2** are stable for at least 6 months. Compound **3** decomposes slowly at room temperature in the solid state, forming a less soluble white powder. However, it was possible to store the compound without any decomposition for at least 3 months at −20 °C as evidenced by ^{1}H NMR.

X-ray Crystallographic Results. The ORTEP structural plot for *S*,*S*-**1** is presented in Figure 1. Crystallographic data and interatomic bond lengths and angles are provided in Tables 1 and S2, respectively. The coordination environment of the silicon atom in *S*,*S*-**1** is a distorted trigonal bipyramid. The methoxy oxygen and the nitrogen atoms occupy the apical positions. Two oxygen atoms and one carbon atom originating from the atrane moiety define the equatorial plane of the trigonal bipyramid of *S*,*S*-**1**. Despite the structural similarities between *S*,*S*-**1** and methoxy{*N*,*N*′,*N*″-2,2′,3-[bis-(ethanolato)(propyl)]amino}silane, the Si−N bond length (2.2437(8) Å) of the former is significantly larger than the respective distance of the latter compound (2.223 Å)[30] and similar to the bond lengths observed for alkyl−carbasilatranes (2.243−2.336 Å).[31−33] Steric interactions originating from the presence of the methyl groups C_8 and C_9 in *S*,*S*-**1** may be the reason for the observed Si−N elongation.

This particular carbasilatrane has three five-membered chelate rings that can be arranged in two different ways. Chart 1 shows the absolute configurations of the molecules. The Δ- and Λ-forms have a right- and left-handed propeller structure, respectively.[34−37] The absolute configuration of the compound in the crystal unit is the Λ-*S*,*S*-**1** (as defined in Chart 1).

Assignment of ^{1}H, ^{13}C, and ^{29}Si NMR Spectra for 1−3 in $CDCl_3$. The solution structures of **1**−**3** were investigated by ^{1}H, ^{13}C, and ^{29}Si NMR spectroscopy in $CDCl_3$. Chemical shifts, coupling constants, and assignments of selected peaks of the compounds are listed in Table 3. The numbering and all possible geometrical configurations of **1**−**3** that may be formed from their synthesis reactions are shown in Chart 1.

The reaction of the racemic epoxides (propylene oxide and glycidol) with (3-aminopropyl)trimethoxysilane leads to the formation of four couples of enantiomeric carbasilatranes, Λ-*S*,*S*-/Δ-*R*,*R*-, Λ-*R*,*R*-/Δ-*S*,*S*-, Λ-*S*,*R*-/Δ-*S*,*R*-, and Λ-*R*,*S*-/Δ-*R*,*S*-. Because Λ- and Δ-configurations interconvert rapidly through a propeller mechanism,[37] Λ-*S*,*S*-/Δ-*R*,*R*- and the Λ-*R*,*R*-/Δ-*S*,*S*- are not distinguishable by NMR spectroscopy. Thus, only three nonequivalent sets of peaks are expected to appear in the NMR spectra of **1** or **2**. On the other hand, two couples of enantiomers, Λ-*S*-/Δ-*R*- and Λ-*R*-/Δ-*S*-, may be formed from the reaction of diethanolamine with racemic (3-glycidoxypropyl)trimethoxysilane. Consequently, only one set of peaks is expected for **3** because of the fast Λ-/Δ-interconversion.

It is important to note here that the kinetics of **1**−**3** were studied by variable-temperature ^{1}H (VT) and 2D {^{1}H} NMR EXSY spectroscopy at a temperature range −65 to 150 °C in $CDCl_3$ (low temperatures) or CD_3CN and dmso-d_6 (high temperatures). These spectra did not show any separation between the Λ and Δ isomers, indicating that even at −65 °C the Λ-/Δ-interconversion is very fast. On the other hand 2D {^{1}H} EXSY spectra did not show any cross-peaks between the protons of the atrane chelate rings even at 150 °C in dmso-d_6, indicating that these molecules are inert toward the opening of the rings.

The ^{29}Si NMR spectrum of **1** in $CDCl_3$ solution revealed three signals at −61.4, −62.4, and −63.8 ppm with ratio 3:2:5, respectively. The larger peak at −63.8 ppm is attributed to the Λ-*S*,*S*-**1**/Δ-*R*,*R*-**1** and the Λ-*R*,*R*-**1**/Δ-*S*,*S*-**1** isomers. The correct assignment of this peak was facilitated by comparing these silicon chemical shifts with those observed in the ^{29}Si NMR spectra of the pure *S*,*S*-**1** and *R*,*R*-**1** compounds in $CDCl_3$. The other two peaks at −62.4 and

(30) Kemme, A. A.; Bleidelis, Y. Y.; Zelchan, G. I.; Urtane, I. P.; Lukevits, E. Y. *Zh. Strukt. Khim.* **1977**, *18*, 343.
(31) Boer, F. P.; Turley, J. W. *J. Am. Chem. Soc.* **1969**, *91*, 4134.
(32) Hencsei, P.; Kovacs, I.; Parkanyi, L. *J. Organomet. Chem.* **1985**, *293*, 185.
(33) Parkanyi, L.; Fulop, V.; Hencsei, P.; Kovacs, I. *J. Organomet. Chem.* **1991**, *418*, 173.
(34) Tasaka, M.; Hirotsu, M.; Kojima, M. *Inorg. Chem.* **1996**, *35*, 6981.
(35) Chandrasekaran, A.; Day, O. R.; Holmes, R. R. *J. Am. Chem. Soc.* **2000**, *122*, 1066.
(36) Timosheva, N. V.; Chandrasekaran, A.; Day, R. O.; Holmes, R. R. *Organometallics* **2001**, *20*, 2331.
(37) Timosheva, N. V.; Chandrasekaran, A.; Day, R. O.; Holmes, R. R. *Organometallics* **2000**, *19*, 5614.

−61.4 ppm are assigned to *S*,*R*-**1** and the *R*,*S*-**1**, respectively. These assignments were further confirmed by 2D {^{1}H} NOESY spectroscopy and are discussed in the following section. The ^{29}Si NMR spectrum of **2** in $CDCl_3$ solution revealed also three signals at −60.8, −62.6, and −63.6 ppm in the ratio 1:2:4, respectively, originating from the *R*,*S*-**2**, *S*,*R*-**2**, and *S*,*S*-**2**/*R*,*R*-**2** isomers, respectively. In contrast, the ^{29}Si NMR spectrum of **3** in $CDCl_3$ gave only one peak at −68.0 ppm, originating from the Λ-*S*-**3**/Δ-*R*-**3** and the Λ-*R*-**3**/Δ-*S*-**3** isomers as expected.

Correlation plots of the ^{29}Si chemical shift with the Si−N donor distance of silatranes have shown an upfield shift in the ^{29}Si value upon increasing the donor coordination.[34,35,37] Such correlation plots cannot be applied to the present molecules because of the lack of crystallographic data for this type of carbasilatrane.[30] A tendency that has been observed for other types of silatranes is that as the steric hindrance of substituents becomes larger, the signals are shifted to lower field.[34] A similar tendency is observed for **1** and **2**, in which the peaks of the sterically hindered *R*,*S*- and *S*,*R*-isomers appeared at lower field compared to the signal of the less hindered *S*,*S*- and *R*,*R*-isomers (Chart 1).

Due to fast Λ-/Δ- interconversion, the *R*,*S*- and *S*,*R*-isomers have a symmetry plane defined by the Si−C−C−C−N ring. Thus, only seven nonequivalent carbon nuclei are expected for each of these molecules, three from the Si−CH_2−CH_2−CH_2−N ring, three from the two Si−O−CH(X)−CH_2−N rings (X = −CH_3, −CH_2OH), and one from the −OCH_3 group. On the other hand, *S*,*S*- and *R*,*R*-enantiomers do not possess any element of symmetry and they contain 10 nonequivalent aliphatic carbons. Excluding the signals from $CDCl_3$, the ^{13}C NMR spectrum of **1** revealed 24 peaks (Table S3), exactly the number expected for the three isomers shown in Chart 1, seven for *R*,*S*-, seven for *S*,*R*-, and 10 for *S*,*S*-/*R*,*R*-. Additional proof for the correct assignments was acquired from the ^{13}C NMR spectra of the pure *S*,*S*-**1** or *R*,*R*-**1**. Each of these spectra revealed 10 signals as expected. These experimental findings are in agreement with the asymmetric structure of *S*,*S*-**1** determined in the solid state by crystallography (Figure 1). A similar type of ^{13}C NMR spectrum was observed for **2** indicating that the solution structures of the isomers of this molecule are similar to those of **1**. The ^{13}C NMR of **3** gave 10 signals (Table S3), six peaks originating from the Si−C−C−C−O−C−C(OH)−C−N ring, three from the carbon atoms of the two diastereotopic Si−O−C−C−N rings, and one from the −OCH_3 group, supporting the structure shown in Chart 1.

The ^{1}H NMR spectra of the silatranes are complicated with several overlapping peaks due to the presence of the various isomers. 2D {^{1}H} COSY and NOESY NMR spectroscopies were used to clarify the spectra (Figure S1). To accurately calculate the chemical shifts and the coupling constants, *J*, the spectra were simulated using gNMR.[27] The experimental and the simulated spectra of *S*,*S*-**1** are shown in Figure 2 as an example. Chemical shifts, *J* coupling constants, and assignments of the ^{1}H NMR peaks of **1**−**3** are listed in Table S3. The absence of symmetry in the *S*,*S*- and *R*,*R*-isomers of **1** and **2** creates nonequivalent environments around the

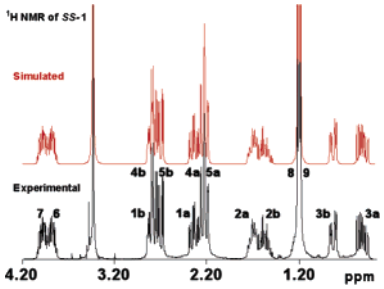

Figure 2. Experimental and simulated by gNMR ^{1}H NMR spectra of **1** in CD_3Cl and assignment of the peaks.

H_a and H_b protons of the Si−C−C−C−N ring (Chart 1), giving separate peaks. In contrast, the respective protons in the *S*,*R*- and *R*,*S*-isomers gave resonances at the same chemical shifts, supporting the symmetric structures proposed above and shown in Chart 1. 2D {^{1}H} NOESY NMR spectroscopy was utilized to distinguish the *R*,*S*-**1** from the *S*,*R*-**1** isomer. More specifically, H_7 and H_6 gave strong NOE cross-peaks with the H_2 and H_1 protons of the *S*,*R*-**1** isomer. These cross-peaks were absent in the case of the *R*,*S*-**1** isomer, because the structure of the molecule does not allow these protons to approach each other (Chart 1). 2D {^{1}H} NOESY NMR spectroscopy was used to distinguish the H_a from the H_b protons. For example, the H_a protons of the *S*,*S*-**1** isomer belonging to atoms C_1, C_2, and C_3 gave strong NOE cross-peaks with the neighboring H_6 proton (Figure S1B). In conclusion, the ^{1}H and ^{13}C NMR spectra of **1**−**3** are in agreement with the proposed solution structures shown in Chart 1.

Aqueous Solution NMR Studies of 1−3. In comparison with triethoxysilanes, the corresponding silatranes are much more difficult to hydrolyze.[38] However, in the presence of acid, the rate of hydrolytic cleavage of silatranes becomes significantly faster. The first and slowest step of the acidic hydrolysis is protonation of the oxygen with simultaneous nucleophilic attack at the silicon.[39] Recent theoretical calculations support the view that O-protonation is kinetically more favorable than N-protonation.[40]

Chemical shifts and assignments of the ^{1}H, ^{13}C, and ^{29}Si NMR spectra of compounds **1**−**3** in D_2O solutions (pHs were 10.6, 10.5, and 9.3, respectively) are listed in Table S4. The hydrolysis reactions of **1**−**3** in aqueous solution at various pHs were monitored by NMR spectroscopy. ^{1}H NMR spectra of **1** and **2** in D_2O gave peaks from all the isomers which have been previously identified in $CDCl_3$ (Table S3). At these alkaline solutions only the CH_3O− group starts to hydrolyze within ∼2 h after dissolution of **1** or **2**. These two molecules are very stable, and for example, even 3 months after dissolution, **1** was only ∼60% hydrolyzed at the CH_3O− group, whereas the atrane rings remained intact. The hydrolytic rate of the CH_3O− group is increased at higher pHs. In contrast, dissolution of **3** in water results in complete hydrolysis of the CH_3O− group and of the atrane ring. The

(38) Voronkov, M. G.; Zelchan, G. I. *Khim. Geterotsikl. Soedin.* **1969**, 450.
(39) Voronkov, M. G.; Emelianov, I. S.; Dyakov, V. M.; Vitkovski, V. Y.; Kapranova, L. V.; Baryshok, V. P. *Khim. Geterotsikl. Soedin.* **1976**, 1344.
(40) Yoshikawa, A.; Gordon, M. S. *Organometallics* **2001**, *20*, 927.

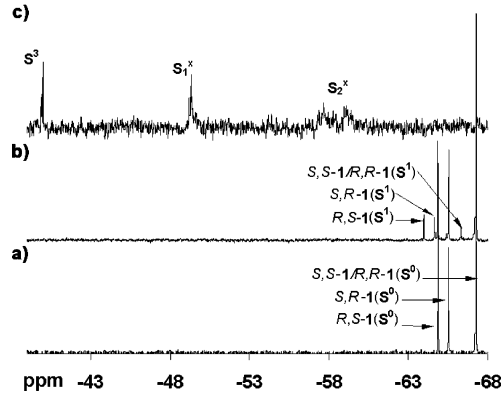

Figure 3. ^{29}Si NMR spectra of 0.05 M of **1** (a) in D_2O for 1 day, (b) in D_2O for 10 days, and (c) 0.10 M CF_3COOH in D_2O for 2 days after dissolution of the compound.

greater instability of **3** compared to **1** and **2** can be attributed to the structural differences of the chelate rings (nine-membered Si−C−C−C−O−C−C(OH)−C−N ring in **3** versus five-membered Si−C−C−C−N ring in **1** and **2**).

Addition of CF_3COOH increases the hydrolysis rates of the carbasilatranes at the atrane rings. The ^{1}H NMR spectra, acquired at various times after dissolution of **1**−**3** in water and after the addition of 2 equiv of CF_3COOH, showed that compounds **1** and **2** are hydrolyzed completely within 3 h after the addition of the acid whereas **3** is hydrolyzed immediately (Figure S2).

^{29}Si chemical shifts are very sensitive to the degree of hydrolysis and condensation of silicon alkoxides. ^{29}Si NMR spectroscopy has been used for the characterization of the species formed from the hydrolysis of alkoxysilanes.[41−43] Figure 3 shows the ^{29}Si NMR spectra and the assignments of the peaks of **1** in D_2O in the absence or in the presence of 2 equiv of CF_3COOH. The ^{29}Si NMR spectrum of a fresh solution of **1** in D_2O contained peaks only from the three isomers *R*,*S*-**1**, *S*,*R*-**1**, and *S*,*S*-/*R*,*R*-**1** (S°). The spectrum of the same solution 10 days later contained three additional peaks originating from the *R*,*S*-, *S*,*R*-, and *S*,*S*-/*R*,*R*-isomers of the species hydrolyzed at the methoxy group (S^1). The −OH groups are more electronegative than the $-OCH_3$ groups and cause hydrolyzed monomeric S^1 species to be shifted to fields lower than that of the S°. Surprisingly *R*,*S*- and *S*,*R*- appear to be hydrolyzed faster than the *S*,*S*-/*R*,*R*-isomers, which may be attributed to the larger steric hindrance of *R*,*S*- and *S*,*R*- compared to *S*,*S*-/*R*,*R*-. The ^{29}Si NMR spectrum of a fresh solution of **1** in D_2O in the presence of 2 equiv of CF_3COOH gave peaks assigned to the fully hydrolyzed open silatranes S^3, $S_1^2S_1^2$, $S_1^2S_2^1S_1^2$, and $S_2^1S_2^1S_2^1$ (Chart 2). The chemical shifts of these peaks are comparable with those usually observed for other trifunctional alkoxy- and hydroxylsilanes. For example (3-aminopropyl)trimethoxysilane gave peaks at approximately −44 ppm for the T^x, −53 ppm for the T_1^x, and −62 ppm for the T_2^x species ($x = 0-3$).[41]

The ^{1}H and ^{29}Si NMR spectra of the CF_3COOH-hydrolyzed **1** and **2**, at various times after pH adjustment around 9, showed that the compounds remained hydrolyzed for 4 days. However, the atrane rings subsequently started to slowly chelate back the silicon atom in the alkaline solution, and 40 days after the pH adjustment more than 60% of the carbasilatrane was re-formed.

Hydrolyses of 1−3 in the Presence of Vanadate. The hydrolyses of **1**−**3** in alkaline aqueous vanadate solutions (pH = 9) at 25 and 80 °C were followed by ^{1}H and ^{51}V NMR spectroscopy. The Si resonances were not observed in the vanadate solutions by ^{29}Si NMR spectroscopy because of the broadening caused by the ^{51}V−^{29}Si coupling.[26] Addition of vanadate in the aqueous solutions of carbasilatrane at 25 °C results in increase of the silatrane hydrolysis rates (both methoxy and atrane hydrolysis) and the generation of new vanadium species (vanadosilicates and vanadium chelate complexes) as evidenced by ^{51}V NMR spectroscopy. The formation of the vanadium chelate complex with concomitant ring opening of *S*,*R*-**1** is shown in eq 2.

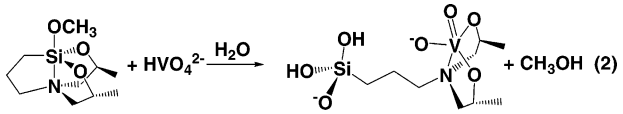

The measurements of the amount of vanadium chelated complexes versus time by ^{51}V NMR spectroscopy show that these solutions need more than 5 days to reach equilibrium at room temperature (Figure 4). Elevation of the temperature of the solutions up to 80 °C increases hydrolysis rates, favoring the formation of higher nuclearity vanadosilicates.

ESI-MS Studies of 1−3. The speciation of **1**−**3** in aqueous solutions was also studied by ESI mass spectroscopy. Spectra collected 30 days after the dissolution of **1** in a H_2O/CH_3OH (1:1) solution are shown in Figure 5. The mass spectra of these compounds support opening of the atrane ring and partial oligonucleation of the silicates in agreement with the NMR spectra. Despite the very slow reactivity of carbasilatranes in H_2O, MS shows formation of a number of mononuclear and dinuclear species in these solutions (Chart 2). The dinuclear species were not detected in the ^{29}Si NMR spectra of this solution probably because they exist in small quantities. H_2O/CH_3OH solutions of **1** acidified with CF_3COOH were found to contain trinuclear oligomers as well (Chart 2). The nuclearity of the species formed in these solutions increased with time.

Characterization of Vanadium(V) complexes in Aqueous Solutions. Reaction of vanadate either directly with aqueous solutions of the carbasilatranes **1**−**3** or with the CF_3-$COOH$-prehydrolyzed carbasilatranes at pH's 8−10 results in the formation of new vanadium complexes. Totals of 6 and 4 days for the former and the latter solutions, respectively, are needed to reach equilibrium. The equilibrated solutions have similar compositions as revealed by ^{51}V NMR spectroscopy.

(41) Rousseau, F.; Poinsignon, C.; Garcia, J.; Popall, M. *Chem. Mater.* **1995**, *7*, 828.
(42) Innosenzi, P.; Brusatin, G.; Licoccia, S.; Vona, M. L.; Babonneau, F.; Alonso, B. *Chem. Mater.* **2003**, *15*, 4790.
(43) Artaki, I.; Bradley, M.; Zerda, T. W.; Jonas, J. *J. Phys. Chem.* **1985**, *89*, 4399.

Chart 2. Proposed Structures of the Species Identified by ESI-MS of **1**[a]

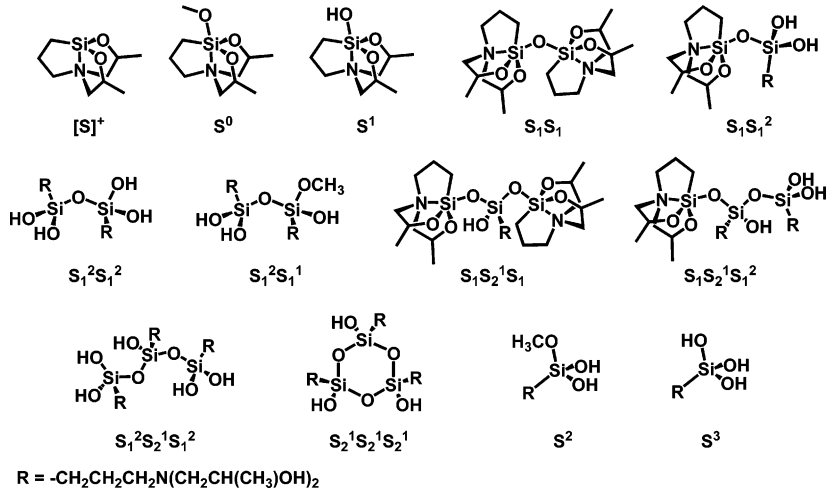

[a] Symbol S_x^y represents the silicon atom that contains x bridged oxygen atoms and y terminal OH groups.

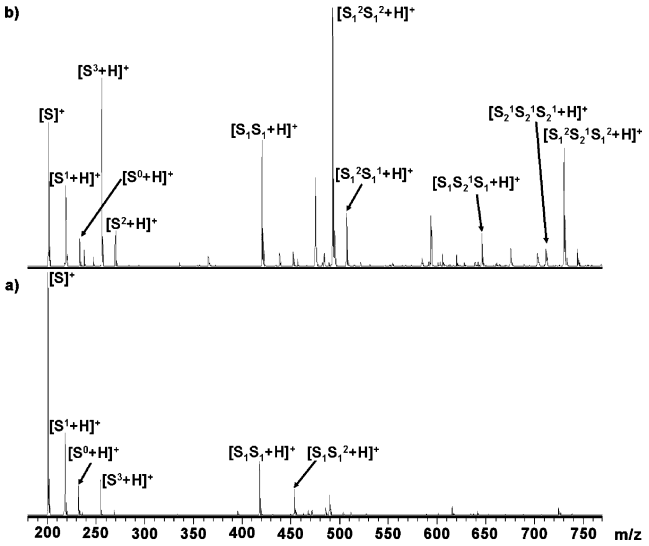

Figure 4. ESI positive-ion mass spectra of H_2O/CH_3OH (1:1) solution containing (a) 0.04 M of **1** and (b) 0.04 M of **1** and 0.2 M of CF_3COOH, 30 days after dissolution.

Figure 6 shows the ^{51}V NMR spectra of aqueous solutions containing equimolar quantities of vanadate and carbasilatrane. Four new peaks in addition to the resonances of the vanadate oligomers (monomer V_1, dimer V_2, tetramer V_4, and pentamer V_5) appeared for these solutions, including the vanadate chelate complex ($\mathbf{V_c}$) with alcohol−aminate group and the vanadosilicates. The vanadosilicates gave one peak at −569.1 ppm, assigned to V_1Si_1 ($[O_3VOSiO(OH)R]^{3-}$), and two broader peaks at −599.4 and −603.8 ppm, assigned to the V_2Si_2 oligomers. The chemical shifts of these peaks are of magnitude similar to those observed for aqueous vanadosilicates derived from the reaction of sodium metavanadate and sodium metasilicate at pH 10.5. In this latter solution, V_1Si_1 ($[O_3VOSiO(OH)_2]^{3-}$) gives one resonance at −569 ppm and the V_2Si_2 a broad resonance at −603 ppm.[26]

The five-coordinated geometry of the vanadate diol or triol aminate negatively charged complexes in aqueous solution is very well documented. ^{51}V NMR spectra of these complexes give peaks in a very narrow range between −478 and −487 ppm.[44−48] Thus, it is reasonable to assume that the peaks at −481.0, −483.7, −487.8, and −484.4 ppm (Figure 6) belong to the five-coordinated dioxovanadium alcohol−aminate chelate complexes, **V-1**, **V-2**, **V-3**, and *S*,*S*-**V-1**, respectively (Chart 3). An important feature of these spectra is the difference between the chemical shift of **V-1** and *S*,*S*-**V-1**. More specifically, the peak of *S*,*S*-**V-1** (−484.4 ppm) is downfield shifted by −3.4 ppm with respect to that of **V-1** (−481.0 ppm). On the basis of ^1H and ^{13}C NMR spectra (described below in detail), it appears that the *R*,*S*-**V-1** isomer consists of about 94% **V-1**. To further investigate this chemical shift difference, the ^{51}V NMR spectra of the aqueous solutions containing vanadate and the ligands **4** and *S*,*S*-**4** were acquired. These two ligands do not contain silicon, but they have the same ligating groups as **1** and *S*,*S*-**1**. The peaks of the five coordinated dioxovanadium alcohol−aminate chelate complexes **V-4** (mainly the *R*,*S*-**V-4** isomer) and *S*,*S*-**V-4** appeared at −484.0 and −481.4 ppm, showing behavior similar to that of the related silicate complexes **V-1** and *S*,*S*-**V-1**. The observed chemical shift difference is probably due to the structural differences between the two complexes that arise from the different positions of the methyl groups in the isomers (Chart 3).

The solution structures of the chelate vanadium complexes ($\mathbf{V_c}$) formed from the reaction of silatranes **1**−**4** with vanadate (**V-1**−**V-4**, respectively) were examined by ^1H and ^{13}C NMR spectroscopy at pH ∼ 9. The chemical shifts of the vanadate chelate complexes and the assignments in these ^1H and ^{13}C NMR spectra are collected in Table 2. The assignments of the signals have been made on the basis of 2D $\{^1H\}$ COSY, 2D $\{^1H\}$ NOESY, and proton-observed 2D $\{^1H,^{13}C\}$ correlations. The spectra contain broad peaks due to the presence of many compounds with similar structure, produced both from the hydrolysis of the silatranes and the complexation of the hydrolyzed silatranes with vanadate. The

(44) Crans, D. C.; Shin, P. K. *J. Am. Chem. Soc.* **1994**, *116*, 1305.
(45) Crans, D. C.; Buoukhobza, I. *J. Am. Chem. Soc.* **1998**, *120*, 8069.
(46) Crans, D. C.; Chen, H.; Anderson, O. P.; Miller, M. M. *J. Am. Chem. Soc.* **1993**, *115*, 6769.
(47) Crans, D. C.; Shin, P. K. *Inorg. Chem.* **1988**, *27*, 1797.
(48) Crans, D. C.; Ehde, P. M.; Shin, P. K.; Pettersson, L. *J. Am. Chem. Soc.* **1991**, *113*, 3728.

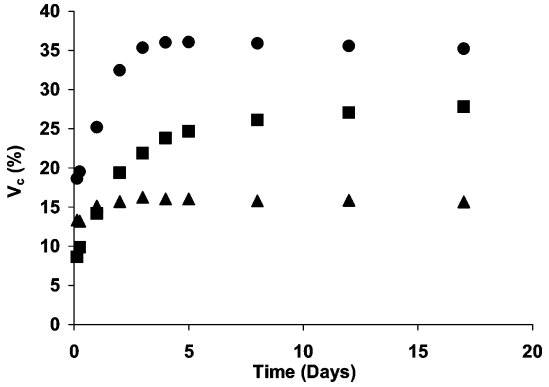

Figure 5. Diagram of the percentage of the vanadate chelate complexes to the total vanadium versus time, calculated from the ^{51}V NMR spectra of solutions in D_2O of 0.05 M of (a) **1**, squares, (b) **2**, triangles, and (c) **3**, circles. These data are the mean values of three separate experiments which were performed for each compound. The deviation was less than 5% of the mean values.

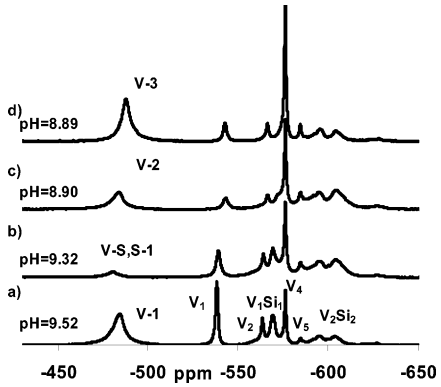

Figure 6. ^{51}V NMR spectra of D_2O solutions containing 0.05 M of CF_3-COOH prehydrolyzed (a) **1**, (b) *S*,*S*-**1**, (c) **2**, and (d) **3** and 0.05 M $NaVO_3$. The pH's of these solutions have been adjusted at pH_{opt} with NaOD.

Chart 3. Proposed Trigonal Bipyramidal and Tetragonal Pyramidal Structures (*S*,*R*- and *S*,*S*-Configurations) in Solution of the $\mathbf{V_c}$-Chelated Complexes on the Basis of ^1H, ^{13}C, and ^{51}V 1D NMR and 2D {^1H} COSY and NOESY Spectra

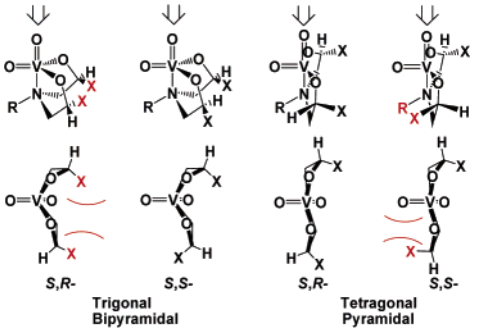

^1H and ^{13}C NMR spectra of the vanadate silatrane aqueous solutions give peaks from the free atrane group, the atrane group coordinated to silicon, and the atrane group coordinated to vanadium.

The solution structure of **V-4** was investigated using the ^{13}C coordination-induced shift (CIS = $\delta_{\text{coordinated ligand}} - \delta_{\text{free ligand}}$) values. The V−TEA/V−TPA (TEA = triethanolamine, TPA = triisopropylamine) complexes for the carbon atoms $C_{6,7}$ exhibit a CIS value of ∼15 ppm.[44] The corresponding CIS value for **V-4** is 13.8 ppm indicating that in solution the vanadium nucleus of this complex has coordination sphere very similar to that of V−TEA/V−TPA (five-coordinated vanadium atom). Because of the broadness of the peaks of the hydrolyzed carbasilatranes, it was not possible to determine the CIS values for the $\mathbf{V_c}$ complexes. However the ^{13}C chemical shifts of **V-4** are similar to the shifts of complexes **V-1** and **V-2** (Table 2), which suggests a five-coordinated V^v for these molecules as well.

Upon coordination of the diol aminate ligands to vanadium, formation of several different stereoisomers is expected, similar to what we had previously observed for compounds **1** and **2**. However, NMR spectroscopy shows all compounds to be diastereomerically pure (∼94% of *R*,*S*-isomer), supporting that the coordination of the diol−aminate ligands on vanadium(V) atom is stereoselective.

The stereochemistry of the vanadium chelate complexes can be unequivocally assigned by the NOEs from the $H_{6,7}$ to the protons of the propyl chain. The 2D {^1H} NOESY spectrum of **V-1** is reported in Figure 7. The most significant NOE is that of the $H_{6,7}$ protons with the $H_{1a,1b}$ protons of the propyl chain, indicating that the absolute configuration of the asymmetric centers of **V-1** is the C_6(*S*)-C_7(*R*). To confirm that the other stereoisomers do not form stable complexes with vanadate, the reaction mixtures of vanadate with the S,S-**1** or the *R*,*R*-**1** isomers were examined by ^{51}V, ^{13}C, and ^1H NMR spectroscopy. The spectra of these solutions showed that only a very small quantity of complexed vanadate is present (4.6% *S*,*S*-**V-1**) (Figure 6), in accordance with our NOE results. **V-2** and **V-4** gave similar cross-peaks in the 2D {^1H} NOESY spectra, indicating that these complexes have C_6(*S*)-C_7(*R*) configuration similar to that of **V-1**.

Relative Stabilities and pH Dependence of the Vanadium Complexes. The stability of these complexes varies with the ligand and with the reaction conditions; among them the pH plays a particularly important role. Diagrams of [$\mathbf{V_c}$]/[V_1] versus pH gave bell type curves, which are well-known for alcohol−aminate vanadium(V) complexes.[45] The optimum pH (pH_{opt}, pH of higher complex stability) for each vanadium(V) complex was estimated from these diagrams and is listed in Table 3. The pH_{opt} values for these complexes ranged from 8.5 to 9.5, which is close to the optimum pH (8−9) obtained for simpler alcohol−aminate vanadium(V) complexes.[45] To investigate the stoichiometry and stability of the complexes, the amount of complex in a series of solutions containing variable vanadate and ligand concentrations at optimum pH was measured by ^{51}V NMR. The plot of [**V-4**] versus [V_1][**4**] gave a straight line, which proves that the formed complex is mononuclear. In contrast, the respective plots of the chelate vanadate complexes with carbasilatranes were not linear. The lack of linearity is probably due to the existence of several other equilibria between the silicates and vanadate that could not be accurately observed due to the overlap of the peaks in the ^{51}V spectra. Excess of silatrane in solution results in the formation of more chelate complex $\mathbf{V_c}$, whereas excess of

Table 2. ^{1}H NMR, ^{13}C NMR, and ^{51}V NMR Chemical Shifts of $\mathbf{V_c}$ Chelate Complexes of Vanadium(V) with Carbasilatranes

atoms	*S*,*S*-**V-1**/*R*,*R*-**V-1**	*R*,*S*-**V-1**/*S*,*R*-**V**-1	*R*,*S*-**V-2**/*S*,*R*-**V**-2	**V-3**	**V-4**	*S*,*S*-**V-4**
C_1, H_1[a]		54.83, 3.14	54.81, 3.18	79.80	54.07, 3.15	
C_2, H_2[a]		18.63, 1.64	19.29, 1.74	20.45	17.42, 1.64	
C_3, H_3[a]					11.47, 0.89	
$C_{4,5}$, $H_{(4,5)a}$, $H_{(4,5)b}$[a]		66.15, 2.15, 3.32	64.32, 2.32, 3.50	70.59, 2.79	66.15, 2.13, 3.39	2.4, 2.7
$C_{6,7}$, $H_{6,7}$[a]		76.34, 4.70	80.87, 4.57	52.84, 4.03	76.30, 4.67	4.6
$C_{8,9}$, $H_{(8,9)a}$, $H_{(8,9)b}$[a]		20.56, 1.14	20.54, 3.48−3.79		20.08, 1.05	
$J_{(4,5)a-(4,5)b}$[b]					11.46	
$J_{6,7-(4,5)a}$, $J_{6,7-(4,5)b}$,					11.46, 2.69	
$J_{6,7-(8,9)a}$, $J_{6,7-(8,9)b}$[b]					9.39[c]	
^{51}V[a]	−481.0	−484.4	−483.7	−487.8	−484.0	−481.4

[a] Chemical shifts in ppm. [b] H_i-H_j coupling constants in Hz. [c] $J_{6,7-(8,9)a} = J_{6,7-(8,9)b}$.

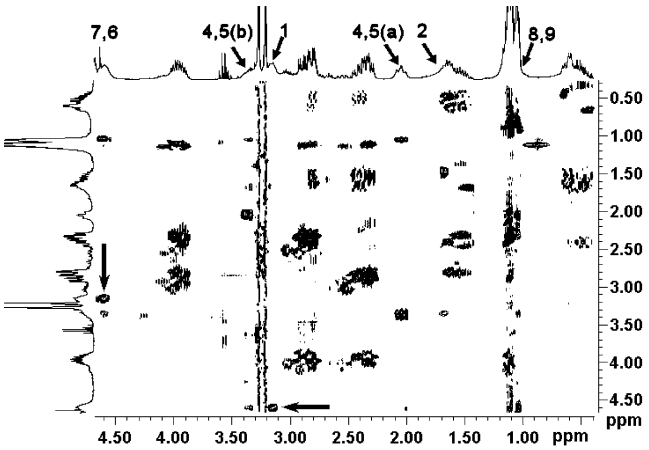

Figure 7. 2D {^{1}H} NOESY spectrum of a D_2O solution containing 0.05 M **1** and 0.05 M $NaVO_3$ at pH = 9.3, at 25 °C using mixing time t_m = 300 ms. The solution has been allowed to equilibrate for 7 days. The numbers in the 1D ^{1}H NMR on the top represent the protons of the *S*,*R*-**V-1** chelate complex. The two arrows in the 2D show the cross-peaks of the NOE interaction between the protons $H_{7/6}$ and H_1.

Table 3. Stability of the Alcohol Aminate Vanadium(V) Complexes **1**−**4**[a]

complex	$\delta(^{51}V)$ (ppm)	$\mathbf{V_c}$ (% to the tot. V)	pH_{opt}
V-1	−484.4	23	9.52
S,*S*-**V-1**	−481.0	4.6	9.32
V-2	−483.7	15	8.90
V-3	−487.8	33	8.89
V-4	−484.0	45	8.90
S,*S*-**V-4**	−481.4	20	8.90

[a] The reactions in this work were studied at 50 mM concentrations of silatranes and 50 mM vanadate. The NMR spectra were acquired 4 days after the preparation of the solutions.

vanadate favored the higher nuclearity vanadosilicates V_2Si_2 (Figure S3).

It has been previously shown that the pK_a of the protonated amino−alcohol and the alkyl substitution on the ligand are important factors that control the stability of the alcohol−aminate vanadium(V) complexes.[45] For example MeDEA (pK_a = 8.52) forms more stable complexes than DEA and EtDEA (pK_a = 8.88 and 8.66, respectively). The presence of an extra chelating functionality (V−TPA, V−TEA), even when it is pendant in aqueous solution,[44] may contribute to the stability of the vanadium(V) complex. $\mathbf{V_c}$ complexes formed from the reaction of vanadate with the mixture of diastereoisomers of the carbasilatranes appear to follow similar stability rules, with stability order **V-3** > **V-2** ∼ **V-1** (Table 3). However the stabilities of the vanadium(V) complexes **V-1** and **V-2** comprise the stabilities of all vanadium isomers formed from the reaction of vanadate with the mixture of *S*,*S*-, *R*,*R*-, *R*,*S*-, and *S*,*R*-isomers of **1** or **2**, respectively. The concentrations of *S*,*S*/*R*,*R*-**V-1** in the aqueous solution containing equimolar quantities (0.050 M) vanadate and **1** at pH_{opt} were found to be 15 times smaller than that for *S*,*R*-**V-1**, whereas the *R*,*S*-**V-1** was not detected as evidenced by multinuclear NMR spectroscopy.

Apparently this large stability difference between the stereoisomers can be attributed to neither the electron donation by the nitrogen atom nor the pK_a of the ligand nor general solvation effects. It must be attributed to stereochemical factors originated from the different orientation of the substituents X on the ligand stereoisomers (Chart 3). To avoid any possible complications caused by the silicates, similar experiments were conducted using the non-silicate-containing ligands **4** and *S*,*S*-**4**. The concentration of *S*,*R*-**V-4** is 12 times higher than those of the *S*,*S*/*R*,*R*-isomers, supporting the argument that steric factors are responsible for the observed stability differences.

There exist only few oxovanadium complexes with chiral triethanolamine derivatives whose crystallographic characterization has been reported in the literature.[46,49,50] These complexes exhibit approximately trigonal bipyramidal coordination geometry, with the nitrogen and terminal oxo atoms in axial positions. In all these studies the ligands were found to be homochiral in the solid state. Although for the synthesis of oxovanadium(V) tri-2-propanolaminate Crans et al. have used racemic tri-2-propanolamine, most of the precipitate consisted of the homochiral isomer. This indicates that even small substituents, such as Me− groups, control the stereochemistry of these compounds through steric interactions.[46] Unfortunately there have been no crystallographic data on the five-coordinated alcohol−aminate dioxovanadium(V) species to date. However, a trigonal bipyramidal geometry for the dioxovanadium(V) compounds should stabilize the homochiral *S*,*S*- and *R*,*R*-complexes better than the *meso*-isomers, due to steric interactions (Chart 3).

It is possible that the complexes exhibit structures similar to those of the analogous five-coordinated dioxomolybdenum(VI) complexes, *cis*-dioxo(2,2′-oxydiethanolato-*O*,*O*′,*O*″)-

(49) Nugent, W. A.; Harlow, R. L. *J. Am. Chem. Soc.* **1994**, *116*, 6142.
(50) Kemme, A. A.; Bieidelis, Y. Y. *Latv. PSR Zinat. Akad. Vestis, Khim. Ser.* **1976**, 322.

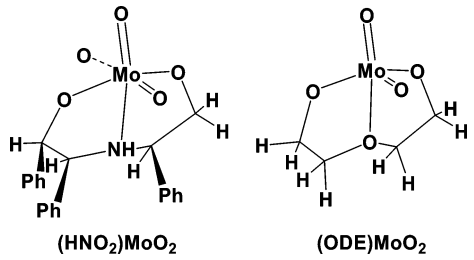

Figure 8. Structures of [(ODE)MoO_2] and [(HNO_2)MoO_2].

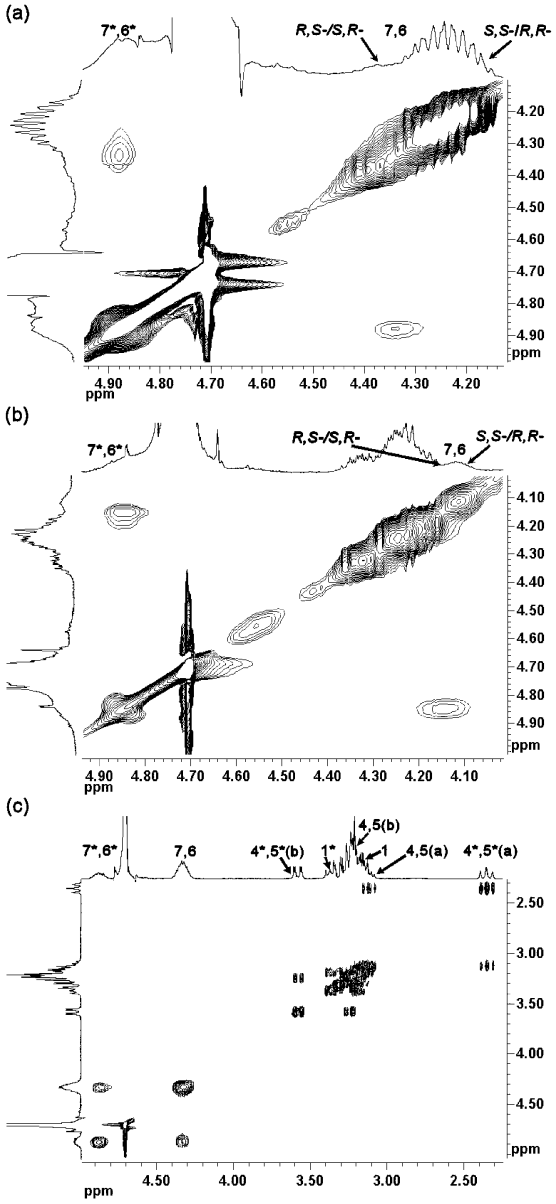

Figure 9. Partial 2D {^{1}H} EXSY spectra of D_2O solutions containing 0.05 M $NaVO_3$ and 0.05 M (a) **1** at pH 9.5, t_m = 250 ms, (b) **2** at pH 9.6, t_m = 360 ms, and (c) **V-4** at pH 9.6, t_m = 700 ms, at 50 °C. The solutions a and b have been allowed to equilibrate for 7 days. Numbers with asterisks show the protons of the chelate complexes $\mathbf{V_c}$, whereas numbers without asterisks are the protons of the carbasilatranes.

oxomolybdenum(VI) [(ODE)MoO_2] and *catena*-((μ_2-oxo)(*N*-(phenyloxyethyl)-*N*-(1,2-diphenyloxyethyl)amine)oxomolybdenum(VI) [(HNO_2)MoO_2] (Figure 8).[51,52] These complexes have a distorted square pyramidal geometry, with the two ethanolate rings and one of the two oxo groups defining the basal plane of the pyramid. Careful examination of this geometry for the *S,S*-, *R,R*-, *R,S*-, and *S,R*-isomers suggests that *S,R*- will be the sterically less hindered structure. In particular, the two methyl groups have more space in the *S,R*- isomer whereas one methyl group in the *S,S*- or *R,R*- and both of them in the *R,S*-isomer are very close to the propyl group, inducing destabilization of these configurations in agreement with the experimental data.

Ligand Exchange of Vanadium Complexes. The exchange reactions between free ligand and the $\mathbf{V_c}$ complexes were studied by 2D {^{1}H} EXSY spectroscopy (Figure 9).[53] The 2D {^{1}H} EXSY experiments were conducted at 25 and 50 °C on samples containing 500 mM vanadate and 500 mM of silatrane. The 2D spectra clearly show exchange between the peaks of $\mathbf{V_c}$ and the resonances of the *R*,S- and *S,R*-carbasilatranes. The resonance of *S,S*-/*R,R*-isomers did not give any cross-peaks due to the very small quantities of the *S,S*-/*R,R*-$\mathbf{V_c}$ complexes present in solution. The exchange rates could not be accurately calculated due to the overlap of the diagonal peaks. However, a rough approximation of the exchange rates, using the ratios of the intensities of the cross versus the diagonal peaks measured in the 2D {^{1}H} EXSY spectra of **V-4** and **V-1**, revealed that **V-4** exchanges faster than **V-1**. This rate difference is explained by the extra step needed to open the carbasilatrane chelate ring of **1** for the alcohol−aminate ligand to ligate vanadate.

Conclusions

In this study we have synthesized carbasilatranes **1**−**3** and their complexes with vanadate. The speciation of **1**−**3** in aqueous solution at alkaline and acidic pH's was investigated by ^{1}H, ^{13}C, and ^{29}Si NMR spectroscopy and ESI mass measurements. **1** and **2** were found to be hydrolyzed slowly only at the methoxy group. The lower stability of **3** in aqueous solution compared to **1** and **2** has been attributed to the different size of the Si−C···N atrane chelate ring (nine- vs five-membered in **1** and **2**). Addition of vanadate results in a significant increase of the hydrolysis rates of carbasilatranes by opening of the atrane moiety. ^{1}H, ^{13}C, and ^{51}V NMR spectra show the formation of vanadosilicates and five-coordinated diol− or triol−aminate dioxovanadium chelate complexes. Although racemic **1** or **2** were used for the complexation of vanadium ion, NMR spectroscopy shows that the *S,R*-isomer comprises 94% of the product formed, whereas the *R,R*-/*S,S*-isomer accounts only for 6%. This stereoselectivity has been attributed to the steric interactions between the methyl or hydroxymethyl groups (for **1** and **2**, respectively) and the carbon atoms of the chelate rings. Examination of the structures and comparison with other literature structures leads to the conclusion that only the

(51) Wilson, A. J.; Penfold, B. R.; Wilkins, C. J. *Acta Crystallogr., Sect. C: Cryst. Struct. Commun.* **1983**, *39*, 329.
(52) Barbaro, P.; Belderrain, T. R.; Bianchini, C.; Scapacci, G. *Inorg. Chem.* **1996**, *35*, 3362.
(53) Crans, D. C.; Jiang, F.; Boukhobza, I.; Bodi, I.; Kiss, T. *Inorg. Chem.* **1999**, *38*, 3275.

tetragonal pyramidal geometry allows stabilization of the *S*,*R*-isomer. In addition, the stability of the chelate complexes of the vanadosilicates varies with pH, concentration, and temperature. The highest concentrations of the chelate complexes were found at pH $\sim$ 9; they increased upon increasing the carbasilatrane concentration. On the other hand, higher temperatures favor the formation of vanadosilicates. 2D {^{1}H} EXSY NMR studies demonstrate that compounds **1**−**4** are involved in an exchange process with the **V-1**−**V-4**, respectively. The exchange rate of this process for **V-1** is slower than the rate for **V-4**. This is attributed to the slow opening of the atrane ring of **1**. In conclusion, pH, concentration, temperature, and the structure of the ligand are important factors that control the speciation in these vanado−carbasilatrane solutions. When using these compounds, alone or in combination with other silicates, to produce sol−gel materials it is clear that, depending on solution conditions and the structure of the ligand, one can produce solid catalysts with widely varying properties. An investigation of the relationship between the vanadate−carbasilatrane solution conditions and the structure of final sol−gel materials as well as the activity and stereoselectivity of the metal ion centers in catalytic oxidation reactions is currently underway.

Acknowledgment. We thank the Cyprus Research Promotion Foundation for funding this work (Program 27/5°PE-2002).

Supporting Information Available: Figure S1, 2D {^{1}H} (A) COSY and (B) NOESY spectra of 0.05 M of *S*,*S*-**1** in $CDCl_3$ at 25 °C and a mixing time for the NOESY t_m of 860 ms, Figure S2, diagram of the percent hydrolyzed carbasilatranes versus time calculated from the ^{1}H NMR spectra of 0.05 M D_2O solutions of (a) **1**, empty rhombus, (b) **2**, filled circles, and (c) **3**, filled squares, in the presence of 0.10 M CF_3COOH, Figure S3, ^{51}V NMR spectra and assignments of D_2O solutions containing various concentrations of vanadate and CF_3COOH-hydrolyzed **1**, Table S1, atomic coordinates ($\times 10^4$) and equivalent isotropic displacement parameters (10^3 Å^2) for **1**, where *U*(eq) is defined as one-third of the trace of the orthogonalized $\mathbf{U}_{ij}$ tensor, Table S2, bond lengths (Å) and angles (deg) for **1**, Table S3, anisotropic displacement parameters (10^3 Å^2) for **1**, where the anisotropic displacement factor exponent takes the form $-2\pi^2[h^2a^{*2}U^{11} + ... + 2hka^*b^*U^{12}]$, Table S4, hydrogen coordinates ($\times 10^4$) and isotropic displacement parameters (10^3 Å^2) for **1**, Table S5, ^{1}H NMR, ^{13}C NMR, and ^{29}Si NMR chemical shifts in $CDCl_3$ and ^{1}H NMR coupling constants for silatrane **1**−**3**, and Table S6, ^{1}H NMR and ^{13}C NMR chemical shifts in D_2O for silatrane **1**−**3**. This material is available free of charge via the Internet at http://pubs.acs.org.

IC050929Q